

Systematic Scrutinization of Vital Factors for the Development of Efficient Cisplatin-Quercetin Loaded Bionanomicelles

Hardik RANA^{1*}

ORCID: 0000-0002-2159-7665

Neha SISODIA¹

ORCID: 0009-0000-4522-5885

Mansi DHOLAKIA²

ORCID: 0000-0001-8141-6013

Vaishali THAKKAR¹

ORCID: 0000-0001-6332-7703

¹Department of Pharmaceutics, Anand Pharmacy College, Opp. Town hall, Anand, 388001, Gujarat, India.

²Faculty of Pharmacy, Dharamsinh Desai University, Nadiad, 387001, Gujarat, India

Corresponding author:

Hardik RANA

Anand Pharmacy College, Anand, Gujarat, India

Tel: +91-8155851416

Tel: +91-2692-2500020

E-Mail:hardikrana1439@gmail.com

Received date : 17.05.2023

Accepted date : 18.05.2024

DOI: 10.52794/hujpharm.1298173

ABSTRACT

The present work aims to optimize and assess the Cisplatin (CIS) and Quercetin (QCT)-loaded biodegradable polymeric nano micelles-Bionanomicelles (BNM). Another objective was to develop a quantitative High-performance thin-layer chromatography (HPTLC) method for estimating CIS and QCT in pharmaceutical dosage form. The aluminum plates coated with silica gel F254 were used for separation of both the drugs employing Toluene: Methanol: Ethyl acetate: DMF: Triethylamine (5:0.5:3.5:1:1 drop % v/v/v/v/v) as mobile phase. The results of the validation parameter indicate that the developed method was precise, accurate, and robust. CIS and QCT-loaded BNM formulated using solvent evaporation technique employing poly lactic-co-glycolic acid (PLGA) 50:50. The Quality by Design (QbD) was accomplished to identify the critical manufacturing attributes and critical process parameters. The formulation was optimized by central composite design using particle size and % encapsulation efficiency as dependent variables. The amount of PLGA and Span were selected as independent variables. Statistically substantial variables were identified using regression analysis and analysis of variance. A diffusion study revealed that optimized nano micelles could sustain the drug release up to 8h. Zeta sizer and TEM confirmed the stability and nano-sized nanoparticles. CIS-QCT BNM was found to be an alternate route to systemic treatment.

Keywords: Cisplatin, Quercetin, HPTLC, PLGA (50:50), Bionanomicelles

1. Introduction

Worldwide, cancer is the second foremost cause of death. Approximately 9.6 million deaths, or one in six demises, occur due to cancer. Eighteen million individuals have cancer, and approximately 30% suffer only from lung cancer. Amongst that, lung cancer mainly occurs in males than females [1]. The expected prevalence of patients with lung cancer in India among males was 0.7 million and among females 0.8 million for the year 2020 [2–6]. Lung cancer is of two types: small cell lung cancer (SCLC) and non-small lung cancer. Approximately 85% suffer from the NSCLC, where adenocarcinoma, large cell carcinoma, and squamous cell carcinoma are the most common [7,8].

Many alternative treatments are available, like surgery, radiotherapy, and chemotherapy for the NSCLC [9]. CIS is considered the first-line treatment for the NSCLC. Currently, CIS is administered via the parenteral route only for immediate action and better therapeutic effectiveness. The significant limitations of the CIS are nephrotoxicity, renal toxicity, cytotoxicity, and many more [10]. The addition of the QCT with the CIS overcame the existing problem of CIS [11,12] QCT is a plant pigment and has potential anticancer and antioxidant activity. It was obtained from many natural sources like fruits and vegetables. QCT has been reported to inhibit CIS-induced nephrotoxicity. QCT attenuated CIS-induced cell death, mitochondrial damage, apoptosis of hair cells, and ultra-structural changes in hair cells [13,14].

Many Classical routes are available for the administration of cytotoxic substances. However, it has several limitations, like requiring a skilled person for the administration, the possibility of dose dumping, less bioavailability, and less specific treatment. A novel inhalation route is preferred to deliver the drug to the lung to avoid such limitations. The lung is widely used as a target site because of numerous advantages like thin alveolar epithelium, larger surface area, high permeation rate through the membrane, and high vasculature, which ultimately leads to high absorption and bioavailability of the substance [15].

Nanocarriers like nano micelles, nanoparticles, liposomes, etc., are fabricated to target the lung. Bionanomicelles have shown promising results for the higher bioavailability compared to other nanocarriers. Nanomicelles are formed using polymer and sur-

factant, entrapping the drug molecules. In contrast, BNMs are made from biodegradable polymers with or without the addition of surfactant. Bionanomicelles have less toxicity and better targeting efficiency than normal nano micelles. It has higher absorption and solubility due to the amphiphilic structure of the BNMs [16,17]. It has more retention time due to the size and leads to less toxicity because of the controlled release of the drug from nano micelles [18,19]. Biodegradable polymers were preferred over non-biodegradable polymers for better control of the drug release, and less toxicity [20,21]. PLGA, Chitosan, and Poly (ϵ -caprolactone) are used for the preparation of BNM. PLGA was chosen for the study due to its controlled release effect, biocompatibility, biodegradability, non-toxic, and better penetration power compared to other excipients. In a nutshell, the present investigation aims to optimize and illustrate CIS and QCT-loaded BNM incorporating progressive data mining techniques.

2. Materials and Methods

Materials

As a gift sample, CIS was obtained from S.G. Biopharm, Himachal Pradesh, India. QCT and PLGA (50:50) were acquired from Merck India Pvt. Ltd., India. The additional analytical grade reagents were used throughout the study.

Fourier Transform Infrared Spectroscopy (FTIR)

The FTIR spectrophotometer assessed the interaction between the CIS, QCT, and PLGA. The spectra of CIS, QCT, and a composite containing CIS, QCT, and PLGA were recorded. The sample (10%) and KBr (90%) were grounded into glass mortar pastel and concerted into the disc. This formulated disc was positioned in a light track, and the spectra were observed in the range of 400 to 4000 cm^{-1} at a resolution of 2 cm^{-1} . KBr was utilized to take background spectra [22–26].

Method Development by HPTLC

Preparation of standard solutions

CIS (10 mg) was precisely weighed and dissolved in 10 ml of 6.8 pH phosphate buffer to prepare a 1000 $\mu\text{g/ml}$ solution. QCT (10mg) was accurately weighed

and was shifted to volumetric flasks (10), solubilized in 10 ml methanol to get a solution containing 1000 µg/ml. 1.4mg/ml 12-oxo Phytodienic acid (OPDA) solution (1ml) and pH 6.8 phosphate buffer solution (1ml) were added to 1 ml stock solution of CIS and QCT, resulting in a light green colored solution. The resulting solution was then cooled to room temperature and diluted with Dimethyl Formamide up to 10ml [27].

Chromatographic procedure

The bands (6 mm) of typical solutions of altered concentrations are located using a Camag Linomat 5 sample applicator on a pre-coated silica gel aluminum Plate 60F254. A twin trough glass chamber was utilized to perform linear uphill development [28]. Toluene: Methanol: Ethyl acetate: DMF: Triethylamine was used as a mobile phase. The saturation time was kept at 20 min at room temperature, and the length for a run was chosen at 8 cm based on the preliminary trials. The HPTLC plates were dehydrated in the air and sprayed using a spraying reagent. The plate was kept in an oven at 85°C; the spot was obtained and subjected to scanning [29]. Camag TLC scanner through WINCATS software was employed for densitometric scanning. All absorbance was measured between 400 to 800nm using slit aspect (6.00 x 0.30 mm, micro) at a scanning rate of 20 mm/s and data perseverance of 100 µm/step. The deuterium lamp emitting a continuous UV light between 200 to 800nm was used as a radiation source. Linear regression statistics were performed to calculate the concentration of both drugs using Minitab software based on the intensities of diffused reflected line and peak area [30–32].

Validation of the developed analytical HPTLC technique

The developed HPTLC technique was validated for the assessment of CIS and QCT. The method is validated for different validation parameters such as linearity [33–35], precision [36,37], accuracy [38,39], LOD [40], LOQ, and specificity considering the concepts of ICH Q2 (R1) guideline [41,42].

Solvent Evaporation Method

The micelle was prepared by rotary flask evaporation under reduced pressure at 300 mmHg. he size of the micelles was adjusted during the same step. The method is also known as the thin-film hydration

method. Weigh the required amount of CIS (10mg), QCT (10mg), and PLGA 50:50 (10-30mg) dissolved in 10 ml of dichloromethane (DCM). Span-80 (0.4-0.8%) was added to the solution and poured into a round bottom flask evaporator for 50 minutes. Allow DCM to evaporate by flash evaporator above their boiling point (50°C) and at 80 RPM. The thin film was formed at the bottom of the flask. The thin film was reconstituted with deionized water to get a suspension of BNM [43–45].

QbD and Risk Estimation Approach

Identifying the Quality Target Product Profile (QTPP) is the leading step of the QbD approach [46]. The quality attributes affecting the product’s quality were gathered. Identifying critical quality attributes is the second and most crucial step in the QbD approach. Identification of significant manufacturing attributes was performed by the Failure Effect Mode Analysis (FMEA) [47,48]. The Fishbone diagram or Ishikawa diagram was constructed by arranging all the manufacturing attributes [49]. The importance of each failure mode was estimated using FMEA. The variable is assessed based on the frequency of occurrence, effect severity, and how simple it can be detected. The critical attributes were identified and studied for the influence of each variable on measured response using the optimization technique [50–52].

The FMEA was performed by calculating each variable’s risk priority number (RPN). RPN score was assigned to each variable based on the OSD approach – event occurrence, the effect’s severity, and the failure mode’s detectability. The arbitrary scale was used to give the score to each parameter. The highest score is given to the most occurring event, most severe effect, difficult-to-detect failure mode, and vice-versa [53].

$$RPN = \begin{bmatrix} 5 \\ 4 \\ 3 \\ 2 \\ 1 \end{bmatrix} O \times \begin{bmatrix} 5 \\ 4 \\ 3 \\ 2 \\ 1 \end{bmatrix} S \times \begin{bmatrix} 1 \\ 2 \\ 3 \\ 4 \\ 5 \end{bmatrix} D \dots \dots \dots \text{Equation 1}$$

Development and Optimization of Processing and Product-Related Parameters

The response surface methodology - Central Composite Design (CCD) is widely used to optimize the formulation as it covers the central and axial points with the least experimental runs. The chosen independent

factors for the design are the amount of PLGA (X_1 , 10-30mg) and Span-80 (X_2 , 0.4-0.8%), whereas the measured responses were %encapsulation efficiency (Y_1 - %EE) and particle size (Y_2) as shown in Table 1. The Design-Expert software (11.0.0) was employed to optimize the final formulation. Based on the software, thirteen experimental runs were performed, as shown in Table 1. The model was developed for each dependent variable to be measured employing multiple linear regression analysis (MLRA) and assessed using one-way ANOVA at 0.05 probability (P) value. The significance of each parameter was determined using the P-value. The terms with higher P-values were considered non-significant and removed for further study [54]. The quadratic model was constructed for each measured response, including the interaction and polynomial terms [55].

Validation of Statistical Analysis for Optimization

The grid search analysis was employed to validate the statistical model. In this method, one optimal and two checkpoint formulations were chosen by random assessment analysis over the whole optimized region. The checkpoint formulations were prepared and assessed for different response parameters. The investigational value of each variable was matched with the anticipated value, and percentage prediction error was premeditated [56,57].

Table 1. Independent variable and their measured responses in Central Composite Design.

Batch No.	X_1 (mg)	X_2 (%)	EE (%)	Particle size (μm)
H 1	5.85786	0.6	72.9	280
H 2	10	0.4	81.2	210
H 3	10	0.8	75.3	270
H 4	20	0.6	88.2	180
H 5	20	0.317157	89.3	150
H 6	20	0.882843	82.2	220
H 7	20	0.6	85.3	220
H 8	20	0.6	82.9	230
H 9	20	0.6	84.2	225
H10	20	0.6	88.6	205
H 11	30	0.8	85.5	110
H 12	30	0.4	94.5	100
H 13	34.1421	0.6	98.3	95

The dose of Cisplatin – 10mg and Quercetin 10mg

Encapsulation Efficiency (%)

One ml suspension of BNM was added in a mixture containing 1 ml ortho phenyl diamine and 2 ml pH 6.8 buffer solution. The solution was heated at 80°C until the color changed from yellow to light blue. The hot solution was allowed to cool at room temperature. The final dilutions were made up of dimethylformamide and measured in HPTLC. Calculate % EE using the following equation: [58,59]

% Encapsulation efficiency =

$$\frac{\text{Experimental drug content}}{\text{Predicted drug content}} * 100 \quad \text{Equation 2}$$

Morphological Studies

The surface morphology of suspension containing CIS- QCT and PLGA (50:50) was analyzed employing a transmission electron microscope (TEM). The thin film of BNM suspension was prepared on a carbon-coated grid, and the additional liquid was discarded. The samples were then analyzed at 120 kV using JEOL 2100F TEM [60].

Zeta Potential Analysis

Zeta potential is an important parameter to identify the stability of nano-sized particles and the intactness of BNM. The Malvern nano zeta sizer was em-

ployed to measure the charge on the particles. Each sample was diluted 20 times with deionized water. The analysis was performed by the zeta sizer based on the Smoluchowski equation [61,62].

Determination of Critical Micelle Concentration

The various concentrations of surfactant solution in the 0.00001-0.1% w/v range were prepared. The KI/I₂ (25 µm) was prepared by solubilizing I₂ (1g) and KI (2g) in 100 ml distilled water. The Iodine solution is added to different surfactant solutions and kept overnight at room temperature. Then, the solution was analyzed at 225nm using HPTLC. The whole procedure was repeated three times to reduce the experimental error. The graph was plotted between the peak area and the amount of polymer. The point at which the sharp change was observed is considered as CMC [63,64].

In-Vitro Diffusion

Polymeric micelle containing CIS and QCT was studied for drug release profile by Franz diffusion cell using pH 6.5 as dissolution media (extracellular cancerous fluid pH). One ml BNM suspension was kept in the donor compartment. Solutions were taken at a programmed time interval and exchanged with fresh media from the receiver compartment. Samples were further suitably diluted and analyzed by the HPTLC method [65].

Aerodynamic Behaviour by Cascade Impactor

The Anderson cascade impactor was employed to identify the aerodynamic behavior of nano micelle. The study is helpful to know the availability of BNM to the lower part of the respiratory tract. The BNM remained in the capsule, any other part of the device, and stages 0-7 were determined using this technique. The seven plates were organized in an ascending order, keeping 0 at the impactor side. In addition, the cascade impactor plates were arranged at both ends. At the side of the base plate, a vacuum and at another end, an induction port was attached. The metered dose inhaler was attached to the instrument. The BNM was sprayed ten times on the attached part. Each plate was removed, rinsed with distilled water, and analyzed for the deposited amount at each plate. The deposition between 2 – 7 plates was considered a respirable fraction [66].

$$\% \text{ Respirable Fraction} = \frac{\text{Amount of drug deposited in lower stage}}{\text{total loaded dose}} \times 100 \dots \dots \text{Equation 3}$$

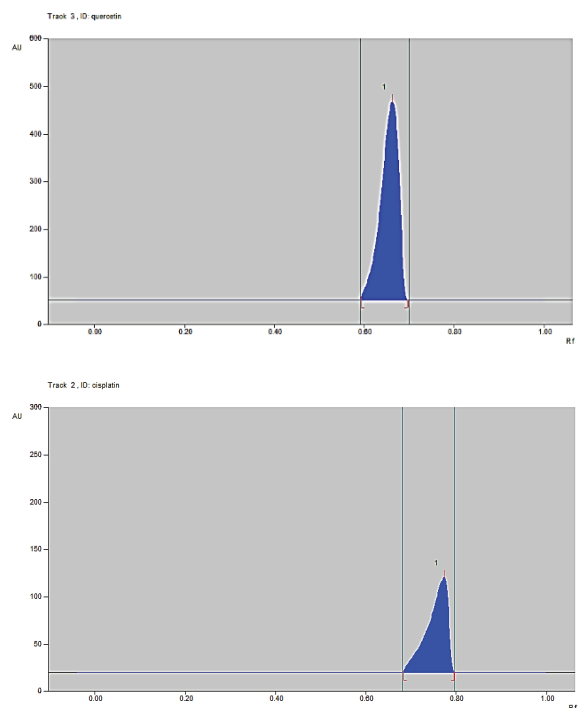
3. Results and Discussion

Mobile Phase Optimization

The mobile phase's polarity is essential to develop a newer HPTLC method, which was confirmed by obtaining a denser band of both drugs in simultaneous estimation. Different mobile phases were used in the study to obtain the dense peak of both the drug, i.e., CIS and QCT. The mobile phase Toluene: Methanol: Ethyl acetate: DMF: Triethylamine (5:0.5:3.5:1:1 drop) was found optimal as a peak having good shape has shown for CIS and QCT.

Detection Wavelength

The wavelength of CIS and QCT was detected in the optimized mobile phase. Derivatization of the compound is necessary to view it at a standard wavelength in the UV chamber for qualitative and quantitative estimation. UV spectra of both drugs after derivatization in Camag TLC scanner IV were recorded to determine the appropriate wavelength. The results indicate that the maximum intensity was observed at 680 nm and 320 nm for both drugs, as depicted in Figures 1A and 1B.



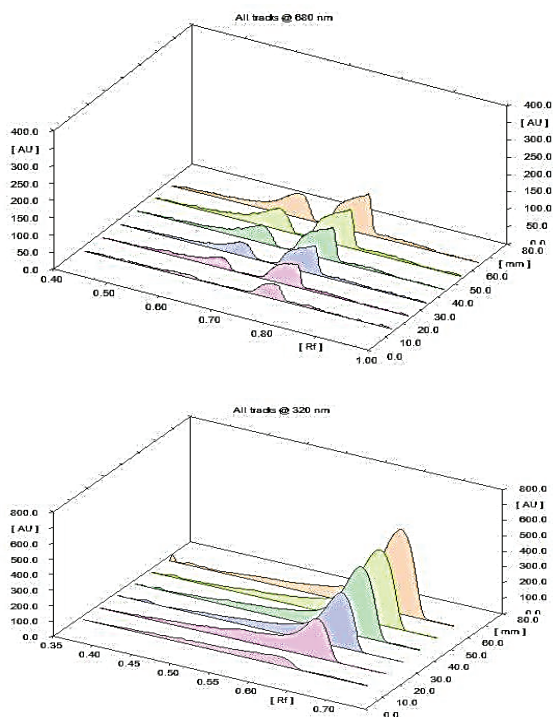


Figure 1. HPTLC chromatogram of (A) CIS and (B) QCT (C) Linearity chromatogram of CIS (D) Linearity chromatogram of QCT.

Method Validation

Linearity

The linearity factor r^2 was used to identify the linearity range. The linearity chromatogram is shown in Figures 1C and 1D. The linearity curve was designed

between the concentration and peak area, as shown in Table 2. Linearity was detected between 4-12 ng/band for both drugs. The r^2 was found to be 0.9954 and 0.9941 for CIS and QCT. The other regression parameters are presented in Table 2.

Precision

Precision was estimated by inter-day as well as intra-day repeatability. Repeatability was assessed for a developed method of CIS and QCT drug. The observations of the repeatability are revealed in Table 3. RSD indicates a high level of precision of the developed method.

Accuracy

The accuracy was calculated from the recovery study at varied stages, 50%, 100%, and 150%, subsequently confounding with a standard. The recovery of CIS was found between 98.74% to 99.91% and 99.95% to 100.27% for QCT, as shown in Table 3.

Specificity

The peak purity of CIS-QCT in BNMs and the standard was determined by comparing spectra, as shown in Figure 2. Peak purity at peak start, peak apex, and peak end, indicating specificity with other interference. The results of peak purity are depicted in Table 3.

Table 2. Calibration study of CIS and QCT by HPTLC method.

CIS		QCT		Constraints	CIS	QCT
Conc. (ng/band)	Area (Mean ± S.D)	Conc. (ng/band)	Area (Mean± S.D)			
0	0	0	0	Calibration range (ng/band)	4-12	4-12
4	2380.36±1.09	4	10450.46±1.19	Linearity equation	$y = 3.7955x + 865.21$	$y = 10.625x + 59993.7$
6	3060.62±0.85	6	12380.62±1.06	R^2 value	0.9954	0.9941
8	4036.36±0.92	8	14080.10±0.89	Slope S.D.	0.3918	0.8182
10	4649.28±0.89	10	16580.10±0.99	Intercept S.D	1.2795	1.1603
12	5381.56±1.24	12	18975.30±0.60	LoD (ng/band)	10.77	4.679
				LoQ (ng/band)	32.65	14.181

(n=5), S.D = Standard deviation

Table 3. Precision, Accuracy, and Specificity results.

Amount of drug applied (ng/ band)	Intra-Day Precision		Inter-Day Precision		Initial quantity of drug (ng/ band)	Accuracy				Specificity		
	Amount of drug found \pm SD ng/band	%RSD	Amount of drug found \pm SD ng/band	%RSD		% of standard added	The total amount of drug	Total amount of drug found (ng/band) \pm SD	Total % of drugs found	r (S, M)	r (M, E)	
CIS												
400	2263.64 \pm 2.29	0.101	2262.96 \pm 1.42	0.062	300	50	450	444.33 \pm 7.03	98.74	Formulation	0.948	0.987
800	4127.02 \pm 2.78	0.067	4126.70 \pm 0.58	0.014	300	100	600	594.66 \pm 5.43	99.11	Standard	0.998	0.989
1200	4927.66 \pm 2.85	0.057	4926.94 \pm 0.013	0.013	300	150	750	749.33 \pm 2.86	99.91			
QCT												
400	6306.70 \pm 1.31	0.020	6304.70 \pm 1.68	0.026	300	50	450	451.11 \pm 1.63	100.22	Formulation	0.989	0.991
800	14061.80 \pm 0.91	0.006	14061.26 \pm 0.82	0.005	300	100	600	601.66 \pm 3.39	100.27	Standard	0.948	0.997
1200	18967.50 \pm 1.17	0.006	18966.00 \pm 0.98	0.004	300	150	750	749.66 \pm 2.49	99.95			

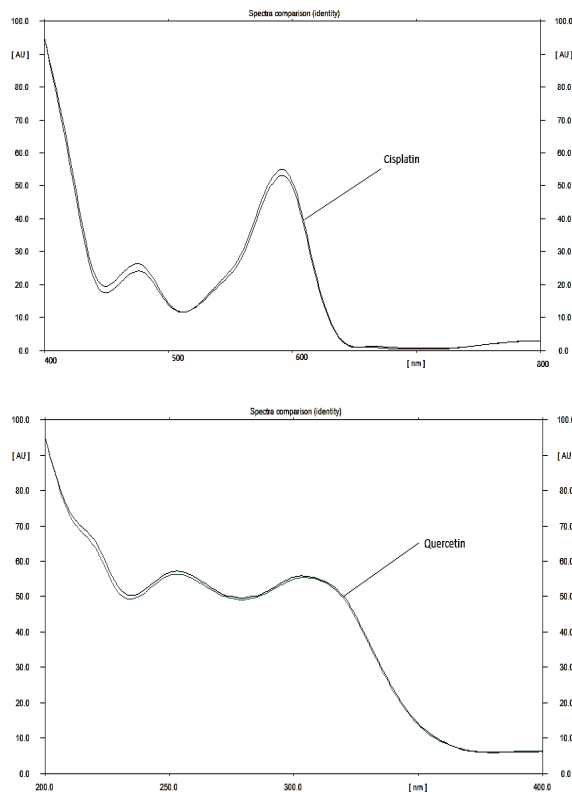


Figure 2. Overlay peak plot spectra of (A) CIS and (B) QCT with the corresponding standard.

LOD and LOQ

The LOD and LOQ of CIS are 10.77ng/band and 32.65ng/band, respectively, whereas LOD and LOQ of QCT were observed at 4.679ng/band and 14.18 ng/band.

Drug-Polymer Compatibility Study through FTIR

The spectra of FTIR of CIS, QCT, and BNMs are shown respectively in Figure 3. The spectra indicate the absence of well-defined interaction between drug and drug and drugs and excipients. Thus, CIS, QCT, and PLGA are compatible with each other.

QbD & Risk Assessment

The first step of the QbD is the identification of QT-PPs for the preparation of CIS-QCT-loaded BNM. The patient-centric QTTPs were identified based on the desired quality of the dosage form to accomplish targeted drug delivery. Different quality parameters are recognized to achieve the targeted profile. The chosen QTTPs were therapeutic indication (lung cancer), target patient population (adults), route of administration (inhalation), site of activity (lower respiratory tract), dosage form (BNMs), solubility (high solubility), dose (10 mg of each). The selected CQAs were Particle Size (<250nm), % Encapsula-

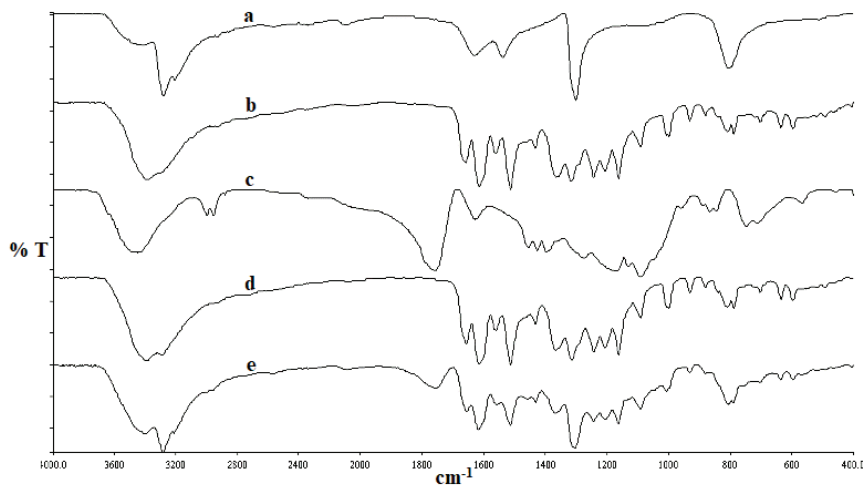


Figure 3. FT-IR spectra of a) CIS, b) QCT, and c) Polymer d) CIS+ QCT, e)BNMs.

tion efficiency (>80%), Diffusion (>75% in 8h) and Zeta Potential (-10 to -30 mV). The parameters affecting the manufacturing of BNM were segregated into the material, man, measurement, environment, machine, and process variables, as revealed in Figure 4. The RPN score employing the FMEA approach is calculated for each parameter and shown in Figure 5. Other than the material variables, the variables were considered to exhibit low risk. All these variables were fixed constant using preliminary trials and previous understanding. The parameters, which show the effect on *in-vivo* product performance, were given a high rank. The RPN score for each variable was used to identify the significant effect on the quality of nanomicelles. The RPN threshold was set to 60. A parameter with more than 60 is considered critical, and vice versa. The variable having a low RPN score (<60) can be excluded from further study[67]. The amount of surfactant and the amount of biodegradable polymer will affect the performance's *in-vivo* and *in-vitro* performance, so they are considered significant. Both the parameters were chosen based on the preliminary study and experience.

Optimization of BNMs

Thirteen experimental trials involving two independent variables, the concentration of PLGA and span 80, were prepared using Design Expert software®. % Encapsulation efficiency (Y_1) and particle size (Y_2) were chosen as responses. The measured responses are depicted in Table 4. The correlation developed between the independent parameters and measured responses using MLRA and ANOVA in the CCD.

The output of MLRA and ANOVA is expressed in the value of the coefficient, F value, and P-value, shown in Table 4.

Influence on Encapsulation Efficiency

A high R^2 Value (0.91) specifies a good fit among the chosen factors and % EE. The suggested quadratic model was found significant as the P-value is 0.0015. The results suggested that two screened factors critically affect %EE. The interaction and polynomial terms are insignificant from the P values for %EE; the inferences can only be concluded from the concerned parameters' main effect. X_1 and X_2 were found critical as it has a P-value of 0.0001. Obviously, as the amount of polymer increases, the % encapsulation efficiency also increases. PLGA is a co-polymer composed of lactic acid and glycolic acid. The inherent structural characteristics and cross-linked structure improved the % EE. The structure's hydrophilicity also affects the entrapment of more drugs due to better interaction with CIS. In addition, it was also observed that the amount of surfactant should be optimum for better encapsulation efficiency. The contour plot (Figure 6A and 6B) for the % EE gives insight into the results. The polynomial equation is given below for the % EE:

$$Y_1 = +85.84 + 7.43 X_1 - 3.12 X_2 - 0.77X_1X_2 - 0.50 X_1^2 - 0.43 X_2^2$$

Equation 4

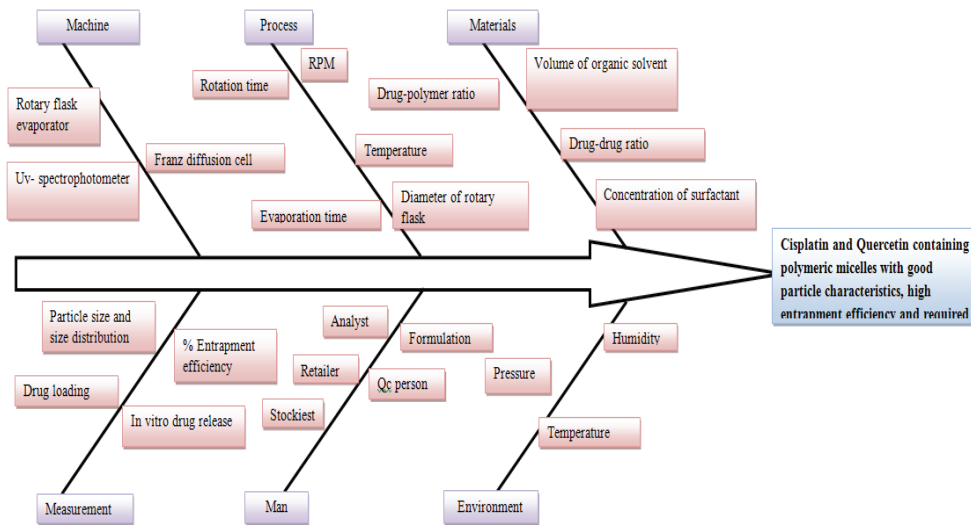


Figure 4. ISHIKAWA Diagram.

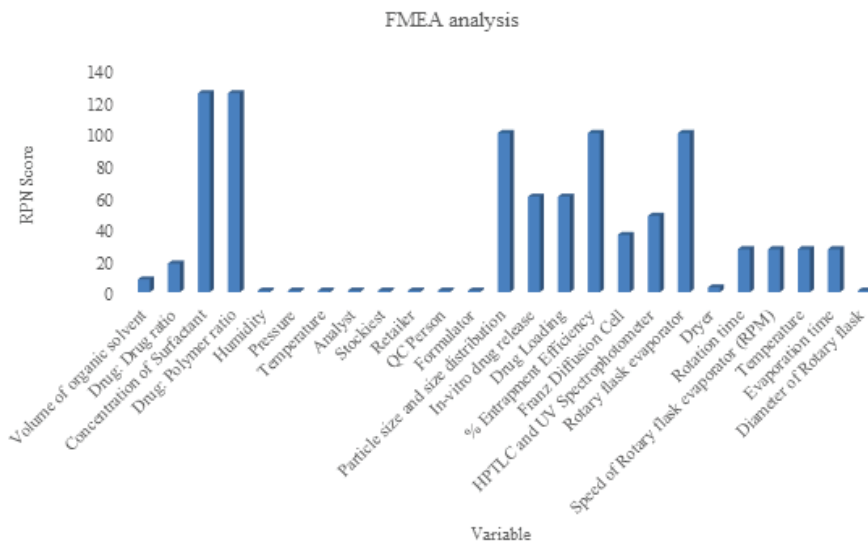


Figure 5. FMEA analysis.

Influence on particle size

A high value of R^2 (0.9528) specifies a good fit between the chosen independent parameters and the particle size. The suggested quadratic model was found significant as the P-value is 0.0001. The results suggest that X_1 , X_2 , X_1^2 , and X_2^2 were critical for the particle size. From this, the conclusion can be drawn that as the concentration of polymer increases, the particle size decreases to some level. The optimum amount of PLGA could control the size of BNMs; above that concentration, the aggregation was observed. The amount of surfactant had a posi-

tive significant effect on the particle size of BNMs. It was mainly due to the aggregation of BNMs due to the higher amount of surfactant. The interaction terms are found to be non-significant, but polynomial terms are found to be significant as the p-value is <0.05 . The contour plot was also plotted for better understanding, as shown in Figures 6C and 6D. A polynomial equation is given below for the particle size.

$$Y_2 = +212.0 - 66.45 X_1 + 21.12 X_2 - 12.50 X_1 X_2 - 15.69 X_1^2 - 16.94 X_2^2 \quad \text{Equation 5}$$

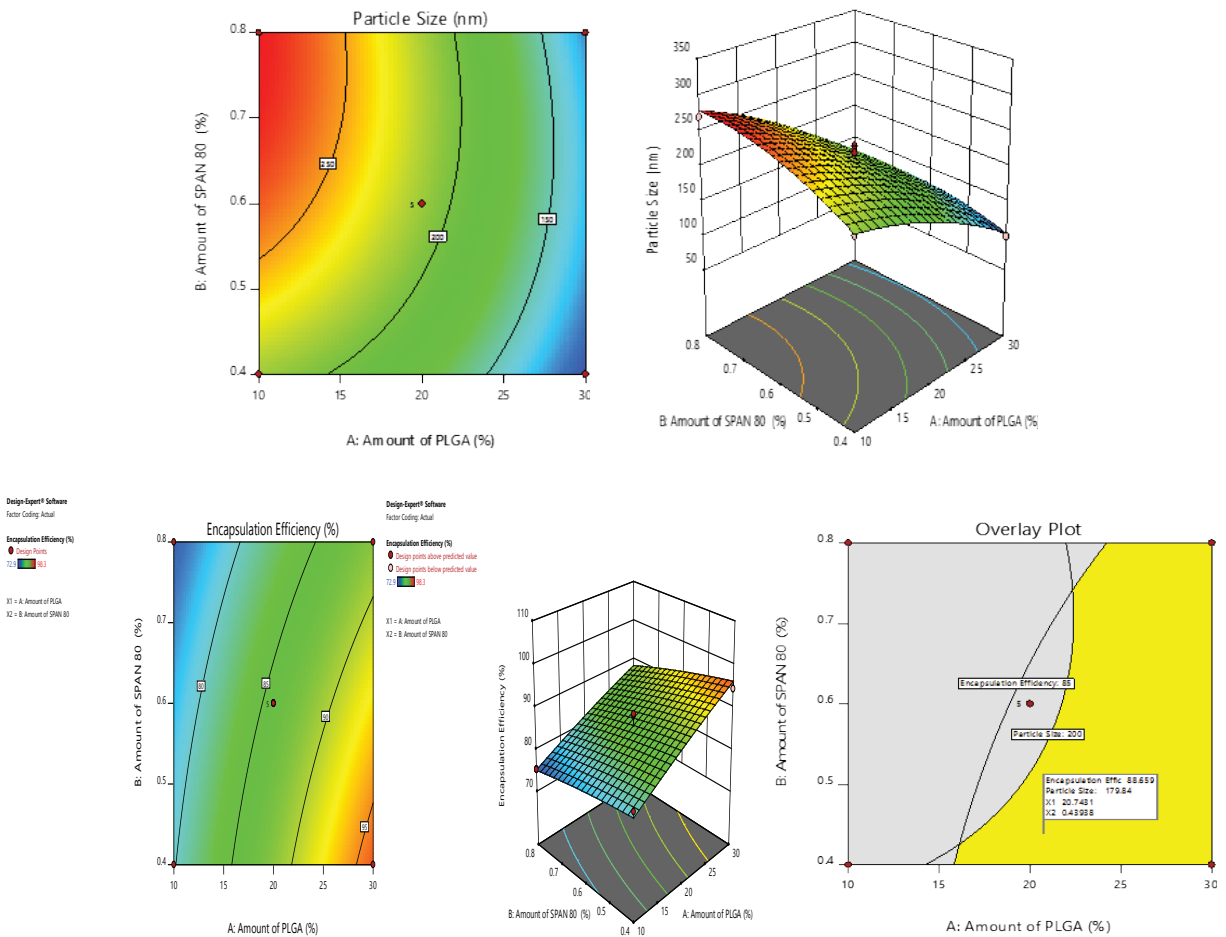


Figure 6. Contour plots of %EE, 3-D plot of %EE, Contour plots of particle size, 3-D plot of particle size, and overlay plot, respectively.

Design Space and its Validation

Design space was determined by overlaying the two contour plots of the measured responses. Figure 6c reveals the overlay plot. The yellow-colored region is the optimum region of the BNM. The researcher is permitted to select any batch within the yellow-colored optimized area. The model validation was performed using the grid search analysis. One optimal composition, as shown in Figure 6c, and two additional compositions were chosen from the design space, formulated, and evaluated for measured responses. The calculated values equated with the projected values of software, and the % prediction error was found to be less than 10, indicating the significant predictability of the chosen model, as shown in Table 4.

Transmission Electron Microscopy

The smaller size of the BNMs was the requirement for the long, systematic circulation and the protection against the removal of BNMs by the reticuloendothelial system (RES). The size of the micelles was observed in the range of 20 to 300nm, which was the desired size for targeting lung cancer. BNMs were found spherical, as shown in Figure 7A. The size and shape of the BNMs were affected by the amount of PLGA and surfactant. The size and shape of the BNMs were not affected by drug loading. A slight change in size was observed after drug loading, which was non-significant. The results indicated that BNMs were not aggregated and remained as an individual entity.

Zeta Potential Analysis

It defines the stability of the formulated nano micelles by measuring the surface charge. The zeta potential of PLGA and drug-loaded micelles was -19.3 with a deviation of $\pm 7.83\text{mV}$, as shown in Figures 7B and 7C. The zeta potential was found to be highly damaging, which was acceptable, and due to this, they remained as individual moieties and stable. The

Determination of CMC

The CMC of the surfactant affects the *in-vitro* and *in-vivo* stability of BNM. The CMC of micelles was found in the range of 0.2 to 1 $\mu\text{g/ml}$. The low observed value indicates higher stability and did not change the structure *in-vivo*. The observed CMC of the optimum composition was at 0.8 $\mu\text{g/ml}$. At this point, the vesicular structure formation started.

In-vitro Diffusion Study

The drug diffusion study of the optimum batch was performed by Franz diffusion cell using extracellular cancerous fluid pH 6.5. At predefined time intervals, samples were collected, suitably diluted, and analyzed at 229 nm using HPTLC. The drug was re-

leased in a controlled manner up to 8h from the CIS-QCT-loaded optimized BNM, depicted in Figure 8A.

Aerodynamic Behavior

The Anderson cascade impactor studied the aerodynamic behavior of BNM. The percentage respirable fraction was found to be 82%, which is desired and indicates the maximum amount of micelles reaching the lung's deep part, like alveoli. The weight that remained on each plate is shown in Figure 8B. Mass Median Aerodynamic Diameter (MMAD) and Geometric Standard Deviation (GSD) were observed at 1.73 μm and 1.49 μm , respectively. Generally, $<0.5 \mu\text{m}$ size micelles are exhaled, whereas having $>0.5 \mu\text{m}$ micelle size impacts the pharynx. So, the micelles having a size $>0.5 \mu\text{m}$ are suitable for delivery into the lung. The resulting data indicate that the maximum amount reaches the lung.

4. Conclusion

The newer, accurate, and precise HPTLC method was developed to estimate Cisplatin and Quercetin. An optimized batch containing CIS, QCT, and PLGA (50:50) is a novel, effective, safe, and patient-friend-

Table 4. ANOVA results and Validation of a model.

Factors	ANOVA results						Validation of Model			
	Y_1			Y_2			Check-point Batches	Optimum batch	Check-point batch I	Check-point batch II
F value	P-value	Coded Coefficient	F value	P-value	Coded Coefficient					
Model	14.15	0.001	7.43	116.54	0.002	+212.00	X_1 (%)	20.74	30.00	30.00
X_1	59.58	0.001	-3.12	11.78	< 0.0001	-66.45	X_2 (%)	0.43	0.80	0.40
X_2	10.50	0.01	-0.78	2.06	0.01	21.12	Predicted Y_1 (%)	88.65	88.43	96.22
$X_1 X_2$	0.32	0.59	-0.51	5.65	0.19	-12.50	Observed Y_1 (%)	85.89	86.28	95.24
X_1^2	0.24	0.64	-0.43	6.58	0.05	-15.69	% Error	3.21	2.49	1.03
X_2^2	0.18	0.69	7.43	116.54	0.04	-16.94	Predicted Y_2 (%)	179.84	121.55	104.29
Lack of fit	1.45	0.35		0.40	0.7597		Observed Y_2 (%)	182.24	129.00	115.00
R^2 Value		0.91			0.9528					

ly formulation. The new formulation overcomes the limitations of traditional treatment. The novel formulation, CIS-QCT loaded bionanomicelles, was delivered directly to the lung, increases the efficacy, reduces the dose, and causes no or minimal side effects with maximum bioavailability. The other ingredients utilized in the study are biocompatible, biodegradable, and FDA-approved. Due to the easy availability of excipients and manufacturing techniques, the scale-up will be accessible at the industry level. The industry can profit better as no such product is available.

Acknowledgment

The author would like to thank S.G. Biopharm, Himachal Pradesh, India, for providing CIS as a gift sample. The author would also like to thank Anand Pharmacy College for providing infrastructure facilities.

Conflict of Interest

The authors confirm that this article's content has no conflict of interest.

Statement of the contribution of researchers

H. R. – Experimental work, designing of work, manuscript writing

N. S. – Experimental work

M. D. – Review and editing of the manuscript

V. T. – Ideation and prototype designing

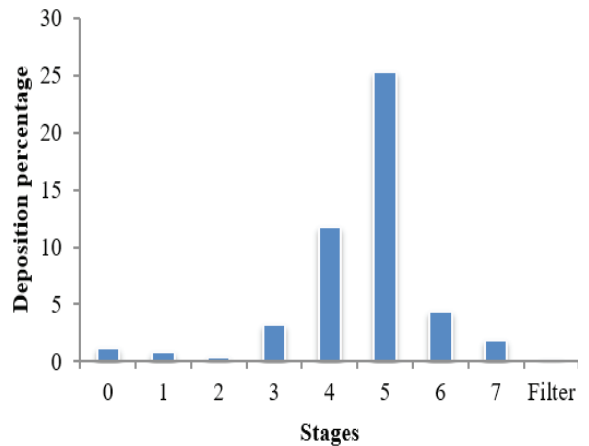


Figure 8.A) *In-vitro* diffusion study of optimized BNM B) Aerodynamic behavior.

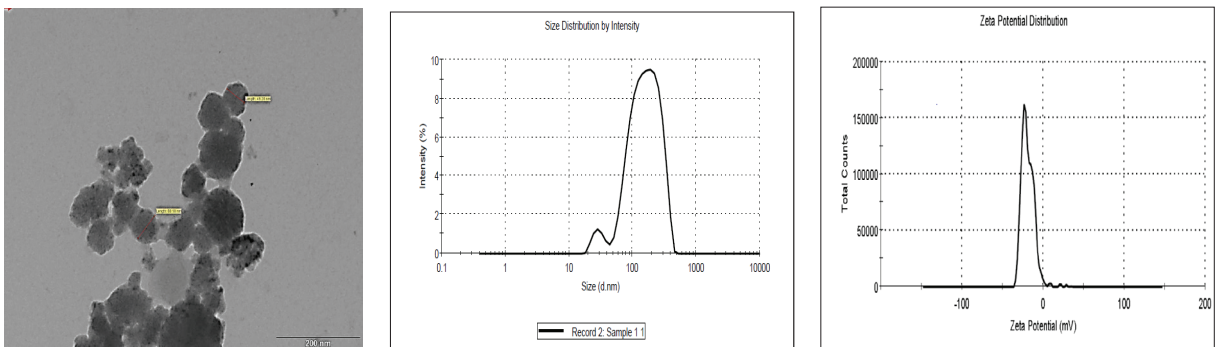


Figure 7. TEM image of Micelles, Size distributions by intensity, and Zeta potential measurement graph, respectively.

References

- World Health Organization. WHO Cancer Report 2020 Global Profile. 2020. Available from: <https://www.who.int/health-topics/cancer>
- Siegel RL, Miller KD, Jemal A. Cancer statistics, 2020. *CA Cancer J Clin*. 2020; 70(1): 7-30. <http://dx.doi.org/10.3322/caac.21590>
- Liu B, Yuan Z, Wei CY. Combined microwave ablation and minimally invasive open decompression for managing thoracic metastasis in breast cancer. *Cancer Manag Res*. 2018; 10:1397-401. <http://dx.doi.org/10.2147/CMAR.S159561>
- SIRO Cinepharm USA. Lung Cancer Focus : India, Tracing the Evolution, Prevalence, Distribution, Etiology, Association, Occurrence, Types, Manifestation & Imoact of Lung Cancer in India. 2015.
- Gujral H, Deulkar K. A review of techniques for lung cancer detection. *Int J Curr Eng Technol*. 2015; 5(3):1597-602.
- Mathur P, Sathishkumar K, Chaturvedi M, et al. Cancer Statistics, 2020: Report From National Cancer Registry Programme, India. *JCO Glob Oncol*. 2020; 6:1063-75. <http://dx.doi.org/10.1200/GO.20.00122>
- Virmani AK, Fong KM, Kodagoda D, et al. Allelotyping demonstrates common and distinct patterns of chromosomal loss in human lung cancer types. *Genes Chromosomes Cancer*. 1998; 21(4):308-19. [http://dx.doi.org/10.1002/\(SICI\)1098-2264\(199804\)21:4<308::AID-GCC4>3.0.CO;2-2](http://dx.doi.org/10.1002/(SICI)1098-2264(199804)21:4<308::AID-GCC4>3.0.CO;2-2)
- Wang J, Nie JJ, Guo P, Yan Z, Yu B, Bu W. Rhodium(I) complex-based polymeric nanomicelles in water exhibiting coexistent near-infrared phosphorescence imaging and anticancer activity *in vivo*. *J Am Chem Soc*. 2020; 142(6):2709-14. <http://dx.doi.org/10.1021/jacs.9b11013>
- Gadgeel SM, Ramalingam SS, Kalemkerian GP. Treatment of lung cancer. *Radiol Clin North Am*. 2012; 50(5):961-74. <http://dx.doi.org/10.1016/j.rcl.2012.06.003>
- Levet V, Rosière R, Merlos R, et al. Development of controlled-release cisplatin dry powders for inhalation against lung cancers. *Int J Pharm*. 2016; 515(1-2):209-20. <http://dx.doi.org/10.1016/j.ijpharm.2016.10.019>
- Dasari S, Tchounwou PB. Cisplatin in cancer therapy: Molecular mechanisms of action. *Eur J Pharmacol*. 2014; 740:364-78. <http://dx.doi.org/10.1016/j.ejphar.2014.07.025>
- Gibellini L, Pinti M, Nasi M, et al. Quercetin and cancer chemoprevention. *Evid Based Complement Alternat Med*. 2011; 2011: 591356. <http://dx.doi.org/10.1093/ecam/neaq053>
- Rau JL. The inhalation of drugs: Advantages and problems. *Respir Care*. 2005; 50(3):367-82.
- Sánchez-González PD, López-Hernández FJ, Dueñas M, et al. Differential effect of quercetin on cisplatin-induced toxicity in kidney and tumor tissues. *Food Chem Toxicol*. 2017; 107(Pt A):226-36. <http://dx.doi.org/10.1016/j.fct.2017.06.047>
- Garbuzenko OB, Mainelis G, Taratula O, Minko T. Inhalation treatment of lung cancer: the influence of composition, size and shape of nanocarriers on their lung accumulation and retention. *Cancer Biol Med*. 2014; 11(1):44-55. <http://dx.doi.org/10.7497/j.issn.2095-3941.2014.01.004>
- Zheng X, Xie J, Zhang X, et al. An overview of polymeric nano micelles in clinical trials and on the market. *Chin Chem Lett* 2021. 32(1):243-57. <http://dx.doi.org/10.1016/j.ccl.2020.11.029>
- Rassu G, Pavan B, Mandracchia D, et al. Polymeric nano micelles based on inulin D α -tocopherol succinate for the treatment of diabetic retinopathy. *J Drug Deliv Sci Technol*. 2021; 61:102286. <http://dx.doi.org/10.1016/j.jddst.2020.102286>
- Wang AZ, Langer R, Farokhzad OC. Nanoparticle delivery of cancer drugs. *Annu Rev Med*. 2012; 63:185-98. <http://dx.doi.org/10.1146/annurev-med-040210-162544>
- Jeetah R, Bhaw-Luximon A, Jhurry D. Polymeric nanomicelles for sustained delivery of anti-cancer drugs. *Mutat Res*. 2014; 768:47-59. <http://dx.doi.org/10.1016/j.mrfmmm.2014.04.009>
- Kanazawa T, Taki H, Okada H. Nose-to-brain drug delivery system with ligand/cell-penetrating peptide-modified polymeric nano-micelles for intracerebral gliomas. *Eur J Pharm Biopharm*. 2020; 152:85-94. <http://dx.doi.org/10.1016/j.ejpb.2020.05.001>
- Jahan F, Zaman S. Mapping the potential of thiolated pluronic based nanomicelles for the safe and targeted delivery of vancomycin against staphylococcal blepharitis. *J Drug Deliv Sci Technol*. 2020; 61:102220. <http://dx.doi.org/10.1016/j.jddst.2020.102220>
- Farhadi E, Kobarfard F, H Shirazi F. FTIR Biospectroscopy investigation on cisplatin cytotoxicity in three pairs of sensitive and resistant cell line. *Iran J Pharm Res*. 2016; 15(1):213-20.
- Kumari A, Yadav SK, Pakade YB, Singh B, Yadav SC. Development of biodegradable nanoparticles for delivery of quercetin. *Colloids Surf B Biointerfaces*. 2010; 80(2):184-92. <http://dx.doi.org/10.1016/j.colsurfb.2010.06.002>
- Vaghani D, Patel A, Thakkar V, Gohel M, Lalji B, Gandhi T. Exploring polymeric nano-particles as targeted pulmonary delivery of rifampicin, ethambutol and ofloxacin against inh-resistant tuberculosis. *J Lung Pulm Respir Res*. 2017; 4(1):1-13. <http://dx.doi.org/10.15406/jlpr.2017.04.00116>
- Mathur P, Saini S, Paul E, Sharma C, Mehtani P. Endophytic fungi mediated synthesis of iron nanoparticles: Characterization and application in methylene blue decolorization. *Curr*

- Res Green Sustain Chem.* 2021; 4:100053. <http://dx.doi.org/10.1016/j.crgsc.2020.100053>
26. Aziz A, Ali N, Khan A, *et al.* Chitosanzinc sulfide nanoparticles, characterization and their photocatalytic degradation efficiency for azo dyes. *Int J Biol Macromol.* 2020; 153:502-12. <http://dx.doi.org/10.1016/j.ijbiomac.2020.02.310>
 27. Basotra M, Singh S K, Gulati M. Development and validation of a simple and sensitive spectrometric method for estimation of cisplatin hydrochloride in tablet dosage forms : Application to dissolution studies. *ISRN Anal Chem.* 2013. <https://doi.org/10.1155/2013/936254>
 28. Motisariya MH, Patel KG, Shah PA. Validated stability-indicating high performance thin layer chromatographic method for determination of ivabradine hydrochloride in bulk and marketed formulation : An application to kinetic study. *Bull Fac Pharm Cairo Univ.* 2013; 51(2):233-41. <http://dx.doi.org/10.1016/j.bfopcu.2013.07.001>
 29. Shah P, Patel J, Patel K, Gandhi T. Development and validation of an hptlc method for the simultaneous estimation of clonazepam and paroxetine hydrochloride using a DOE approach. *J Taibah Univ Sci.* 2017; 11(1):121-32. <http://dx.doi.org/10.1016/j.jtusci.2015.11.004>
 30. Elkhoudary MM, Selim BM, AbdelSalam RA, Hadad GM, El-Gindy A. Development and validation of a simple HPTLC method for the determination of new hepatitis C Subtype 4 antiviral agents in their tablet dosage form. *J Planar Chromatogr Mod TLC.* 2020; 33(1):71-7. <http://dx.doi.org/10.1007/s00764-019-00006-y>
 31. Ahmad W, Husain I, Ahmad N, *et al.* Box-behnken supported development and validation of robust HPTLC Method: An application in estimation of punarnavine in leaf, stem, and their Callus of *Boerhavia diffusa* linn. *J Biotech.* 2020; 10(4):1-10. <http://dx.doi.org/10.1007/s13205-020-2154-1>
 32. Emam AA, Naguib IA, Hassan ES, Abdelaleem EA. Development and validation of RP-HPLC and an ecofriendly HPTLC method for simultaneous determination of felodipine and metoprolol succinate, and their major metabolites in human spiked plasma. *J AOAC Int.* 2020; 103(4):966-71. <http://dx.doi.org/10.1093/jaoacint/qs040>
 33. Thomas AB, Patil SD, Nanda RK, Kothapalli LP, Bho-sle SS, Deshpande AD. Stability-indicating HPTLC method for simultaneous determination of nateglinide and metformin hydrochloride in pharmaceutical dosage form. *Saudi Pharm J.* 2011;19(4): 221-31. <http://dx.doi.org/10.1016/j.jsps.2011.06.005>
 34. Mistry NN, Shah P, Patel K, Hingorani L. Simultaneous estimation of stigmasterol and withaferin A in union total herbal formulation using validated HPTLC method. *J Appl Pharm Sci.* 2015; 5(08):159-66. <http://dx.doi.org/10.7324/JAPS.2015.50825>
 35. Ahmad A, Amir M, Alshadidi AA, Hussain MD, Haq A, Kazi M. Central composite design expert-supported development and validation of HPTLC method: Relevance in quantitative evaluation of protopine in *Fumaria indica*. *Saudi Pharm J.* 2020; 28(4):487-94. <http://dx.doi.org/10.1016/j.jsps.2020.02.011>
 36. Kekre VA, Walode SG. Validated Hptlc Method for Estimation of Curcumin Content in Dietary Supplement. *IJPRS.* 2012; 3(10):3796-800. [http://dx.doi.org/10.13040/IJPSR.0975-8232.3\(10\).3796-00](http://dx.doi.org/10.13040/IJPSR.0975-8232.3(10).3796-00)
 37. Patel RB, Patel MR, Patni NR, Agrawal V. Efinaconazole: DoE-supported development and validation of a quantitative HPTLC method and its application for the assay of drugs in solution and microemulsion-based formulations. *Anal Methods.* 2020; 12(10):1380-8. <http://dx.doi.org/10.1039/C9AY02599E>
 38. Syed HK, Liew KB, Loh GO, Peh KK. Stability indicating HPLC-UV method for detection of curcumin in *Curcuma longa* extract and emulsion formulation. *Food Chem.* 2015; 170:321-6. <http://dx.doi.org/10.1016/j.foodchem.2014.08.066>
 39. Alam P, Ezzeldin E, Iqbal M, *et al.* Ecofriendly densitometric RP-HPTLC method for determination of rivaroxaban in nanoparticle formulations using green solvents. *RSC Advances.* 2020; 10(4):2133-40. <http://dx.doi.org/10.1039/C9RA07825H>
 40. BinduG, Ravi Kiran Suripeddi, Development and validation of HPTLC method for identification and quantification of sterols from leaves of *Erythroxylum Monogynum* Roxb. and *in vitro* evaluation of antioxidant and anti-glycation activities. *S Afr J Bot.* 2021; 137:24-34. <http://dx.doi.org/10.1016/j.sajb.2020.10.005>
 41. Shewiyoo DH, Kaale E, Risha PG, Dejaegher B, Smeyers-Verbeke J, Vander Heyden Y. HPTLC methods to assay active ingredients in pharmaceutical formulations: A review of the method development and validation steps. *J Pharm Biomed Anal.* 2012; 66:11-23. <http://dx.doi.org/10.1016/j.jpba.2012.03.034>
 42. ICH topic Q2 (R1) validation of analytical procedures : Text and methodology. *Int Conf Harmon.* 2005; 1-17. Available from: https://doi.org/http://www.ich.org/fileadmin/Public_Web_Site/ICH_Products/Guidelines/Quality/Q2_R1/Step4/Q2_R1_Guideline.pdf
 43. Hu X, Han R, Quan LH, Liu CY, Liao YH. Stabilization and sustained release of zeelenone, a soft cytotoxic drug, within polymeric micelles for local antitumor drug delivery. *Int J Pharm.* 2013; 450(1-2):331-7. <http://dx.doi.org/10.1016/j.ijpharm.2013.04.007>

44. Szczech M, Szczepanowicz K. Polymeric core-shell nanoparticles prepared by spontaneous emulsification solvent evaporation and functionalized by the layer-by-layer method. *Nanomaterials (Basel)*. 2020; 10(3):5-8. <http://dx.doi.org/10.3390/nano10030496>
45. Jia F, Li Y, Lu J, Deng X, Wu Y. Amphiphilic block copolymers-guided strategies for assembling nanoparticles: From basic construction methods to bioactive agent delivery applications. *ACS Appl Bio Mater*. 2020; 3(10):6546-55. <http://dx.doi.org/10.1021/acsbm.0c01039>
46. Gregg Claycamp H. Perspective on quality risk management of pharmaceutical quality. *Drug Inf J*. 2007; 41(3): 353-67. <http://dx.doi.org/10.1177/009286150704100309>
47. Dave VS, Fahmy RM, Bensley D, Hoag SW. Eudragit® RS PO/RL PO as rate-controlling matrix-formers via roller compaction: Influence of formulation and process variables on functional attributes of granules and tablets. *Drug Dev Ind Pharm*. 2012; 38(10):1240-53. <http://dx.doi.org/10.3109/03639045.2011.645831>
48. Dave VS, Fahmy RM, Hoag SW. Investigation of the physical-mechanical properties of Eudragit® RS PO/RL PO and their mixtures with common pharmaceutical excipients. *Drug Dev Ind Pharm*. 2013; 39(7):1113-25. <http://dx.doi.org/10.3109/03639045.2012.714786>
49. A Review of: "Introduction to Quality Control." By Kaoru Ishikawa. Translated by J. H. Loftus (Chapman and Hall, London, 1991). *Int J Prod Res*. 1992; 30(12):2952-2. <http://dx.doi.org/10.1080/00207549208948202>
50. Stamatis DH. Failure mode and effect analysis FMEA from theory to execution. 2nd ed. Milwaukee: ASQ Quality Press 2003.
51. Mahdizadeh M, Zamanzade E. A new reliability measure in ranked set sampling. *Stat Hefte*. 2018; 59(3):861-91. <http://dx.doi.org/10.1007/s00362-016-0794-3>
52. Zamanzade E, Mahdizadeh M. Using ranked set sampling with extreme ranks in estimating the population proportion. *Stat Methods Med Res*. 2020; 29(1):165-77. <http://dx.doi.org/10.1177/0962280218823793>
53. Fahmy R, Kona R, Dandu R, Xie W, Claycamp G, Hoag SW. Quality by design I: Application of failure mode effect analysis (FMEA) and Plackett-Burman design of experiments in the identification of "main factors" in the formulation and process design space for roller-compacted ciprofloxacin hydrochloride immediate-release tablets. *AAPS PharmSciTech*. 2012; 13(4):1243-54. <http://dx.doi.org/10.1208/s12249-012-9844-x>
54. Gurram RK, Gandra S, Shastri NR. Design and optimization of disintegrating pellets of MCC by non-aqueous extrusion process using statistical tools. *Eur J Pharm Sci*. 2016; 84(1):146-56. <http://dx.doi.org/10.1016/j.ejps.2016.01.021>
55. Bei YY, Zhou XF, You BG, *et al*. Application of the central composite design to optimize the preparation of novel micelles of harmine. *Int J Nanomedicine*. 2013; 8:1795-808. <http://dx.doi.org/10.2147/IJN.S43555>
56. Kollipara S, Bende G, Movva S, Saha R. Application of rotatable central composite design in the preparation and optimization of poly(lactic-co-glycolic acid) nanoparticles for controlled delivery of paclitaxel. *Drug Dev Ind Pharm*. 2010; 36(11):1377-87. <http://dx.doi.org/10.3109/03639045.2010.487263>
57. Singh B, Chakkal SK, Ahuja N. Formulation and optimization of controlled release mucoadhesive tablets of atenolol using response surface methodology. *AAPS PharmSciTech*. 2006; 7(1):E3. <http://dx.doi.org/10.1208/pt070103>
58. Zhang Z, Feng SS. The drug encapsulation efficiency, *in vitro* drug release, cellular uptake and cytotoxicity of paclitaxel-loaded poly(lactide)-tocopheryl polyethylene glycol succinate nanoparticles. *Biomaterials*. 2006; 27(21):4025-33. <http://dx.doi.org/10.1016/j.biomaterials.2006.03.006>
59. Praphakar RA, Munusamy MA, Rajan M. Development of extended-voyaging antioxidant linked amphiphilic polymeric nanomicelles for anti-tuberculosis drug delivery. *Int J Pharm*. 2017; 524(1-2):168-77. <http://dx.doi.org/10.1016/j.ijpharm.2017.03.089>
60. Sugihara K, Nakano S, Koda M, Tanaka K, Fukuishi N, Gemba M. Stimulatory effect of cisplatin on production of lipid peroxidation in renal tissues. *Jpn J Pharmacol*. 1987; 43(3):247-52. [http://dx.doi.org/10.1016/S0021-5198\(19\)43504-X](http://dx.doi.org/10.1016/S0021-5198(19)43504-X)
61. Sezgin Z, Yüksel N, Baykara T. Preparation and characterization of polymeric micelles for solubilization of poorly soluble anticancer drugs. *Eur J Pharm Biopharm*. 2006; 64(3):261-8. <http://dx.doi.org/10.1016/j.ejpb.2006.06.003>
62. Oda CMR, Silva JO, Fernandes RS, *et al*. Encapsulating paclitaxel in polymeric nano micelles increases antitumor activity and prevents peripheral neuropathy. *Biomed Pharmacother*. 2020; 132:110864. <http://dx.doi.org/10.1016/j.biopha.2020.110864>
63. Rana HB, Raj A, Patel A, Gohel M. Preparation, optimization and *in vitro* characterization of cisplatin loaded novel polymeric micelles for treatment of lung cancer. *Int J Res Sci Innov*. 2016; IV(1):431-41.
64. Wei Z, Hao J, Yuan S, *et al*. Paclitaxel-loaded Pluronic P123/F127 mixed polymeric micelles: Formulation, optimization and *in vitro* characterization. *Int J Pharm*. 2009; 376(1-2):176-85. <http://dx.doi.org/10.1016/j.ijpharm.2009.04.030>
65. Singhvi G, Singh M. Review : *In vitro* drug release characterization models. *Int J Pharm Stud Res*. 2011; II(1):77-84.

66. Shrikhande SS, Rao A, Ambekar A, Bajaj AN. Metered dose inhalation formulations of salbutamol sulphate using non-CFC propellant tetrafluoroethane. *Int J Pharm Sci Drug Res.* 2011; 3(4):292-6.
67. Wang J, Kan S, Chen T, Liu J. Application of quality by design (QbD) to formulation and processing of naproxen pellets by extrusion-spheronization. *Pharm Dev Technol.* 2015; 20(2):246-56. <http://dx.doi.org/10.3109/10837450.2014.908300>